Rev. Adv. Mater. Sci. 55 (2018) 69-77

ANNEALING-INDUCED GRAIN ROTATION IN ULTRAFINE-GRAINED ALUMINUM ALLOY

V. N. Danilenko[1], D. V. Bachurin[1,2] and A. A. Nazarov[1]

[1]Institute for Metals Superplasticity Problems of the Russian Academy of Sciences, 39 Khalturin str., Ufa 450001, Russia
[2]Institute for Applied Materials Physics, Karlsruhe Institute of Technology, 76344, Eggenstein-Leopoldshafen, Hermann-von-Helmholtz-Platz 1, Germany

Received: December 22, 2017

Abstract. Results of *in situ* transmission electron microscopic studies of annealing-induced evolution of grain boundary misorientations in ultrafine-grained aluminum alloy Al-4%Cu-0.5%Zr (wt.%) processed by high pressure torsion are presented. An experimental procedure based on the single reflection technique was applied for the measurements of orientations of individual grains before and after annealing that allowed for determining misorientations between them. The measurements revealed that relaxation processes occurring in non-equilibrium grain boundaries during short-time annealing are accompanied by a change of grain boundary misorientations, grain rotation, grain migration as well as grain growth. Obtained results were compared with theoretical studies considering the kinetics of grain rotation in discrete-dislocation as well as continuum approaches.

1. INTRODUCTION

The phenomenon of merging of two neighboring subgrains into one of a single orientation was firstly revealed during recrystallization process by Hu [1]. The growth of the subgrains was accompanied by gradual disappearance of the subboundaries, i.e. by the subgrain coalescence occurring as a result of subgrain rotation. Theoretical substantiation and kinetic analysis of subgrain rotations based on the cooperative climb of grain boundary dislocations was given by Li [2].

Later in 70-80-ths it was demonstrated that a single crystal ball sintered on a single crystal plate of a different crystallographic orientation could rotate and thus reduce interfacial energy [3-5]. Due to an absence of constraints from the neighboring grains, the rotational movement of such metallic balls is facilitated at elevated temperatures and therefore can be measured. It was established that untilting of two crystallites occured by the climb of edge and glide of screw grain boundary dislocations [6,7].

A renewed interest to grain rotation in the last decades is related to a broad investigation of polycrystalline materials with nanometer grain sizes. Numerous experimental and theoretical studies suggest that grain rotation can be considered as a mechanism of plastic deformation, which is often accompanied by grain growth and grain boundary sliding. Grain rotation during deformation process was observed in thin nanocrystalline films of gold [8,9], ultrafine-grained aluminum films [10,11], high-density nanocrystalline gold and copper prepared by the gas deposition method [12,13], nanocrystalline copper obtained by severe plastic deformation method [13], etc. Deformation mechanisms of nanostructured materials involving grain rotation was considered in Refs. [14,15].

Corresponding author: V.N. Danilenko, e-mail: vdan@anrb.ru.

There is an experimental evidence of grain rotation under applied deformation even in coarse-grained polycrystals: aluminum [16-18], high-purity aluminum bicrystals [19], TRIP 800 steel [20], zirconium diboride silicon carbide composite [21], austenite grains in a low-carbon steel [22]. Grain rotation during fatigue crack growth in Al alloys was observed at room temperatures [23] as well as during plasma nitriding of 316L austenitic stainless steel [24]. Authors of [20] consider grain rotation as an additional mechanism resulting in an increase of plasticity of TRIP 800 steel sheet contribution of which is comparable with austenite-martensite transformation.

Grain rotation was experimentally observed during superplastic deformation [25-27]. A theoretical model describing the process of superplastic deformation was proposed by Beere [28], which considers grain rotation accompanying by grain boundary migration. The necessity of taking into account the processes occurring at grain boundaries for analysis of superplastic deformation was emphasized in Ref. [29].

A great achievement in understanding of grain rotation process during deformation is related to an appearance and improvements of experimental techniques, which allow accurate determination of the rotation parameters of the grains. Recently, Margulies et al. [17-30] have proposed the method of *in situ* measurement of grain rotation during deformation based on diffraction with focused hard X-rays and measured rotation of the grains in high-purity aluminum with an average grain size of 300 μm. It was found that grains rotated to angles in the range from 0.5 to 5.5° in the sample subjected to tensile deformation of 6%.

As seen from the review given above, the majority of the cited publications were devoted to a study of grain rotation during deformation process, i.e. as a response to external straining. We are aware of only a few experimental works [1,31,32] where grain rotation during annealing was revealed. Grain rotation in Fe-3%Si monocrystal thin foils after cold rolling was registered by means of gradual disappearance of subboundaries [1]. During *in situ* annealing in a column of high-voltage transmission electron microscope grain rotation in thin foils of Al-6%Ni alloy was determined by a decrease of the number of dislocations in a low-angle grain boundary between two subgrains [32]. Grain rotation in thin columnar gold films during sequential annealing was measured by the changing orientations of twin boundaries within the grains [31]. It should be noted that anneals in Ref. [31] were performed outside the microscope. Thus, in the above-cited works the process of grain rotation was characterized mainly qualitatively.

Grain rotation as a mechanism of changing grain boundary misorientations upon annealing was proposed in Refs. [33-36].

Crystallographic characteristics of large numbers of grain boundaries in polycrystalline materials were measured in nickel [33] by means of the electron back-scatter diffraction method and in nickel-based superalloy [34] using the convergent-beam diffraction. It was established that the ratio of "close packed" low Σ boundaries increases during annealing suggesting rotation of grains toward coincidence site lattice configurations and thus minimizing the system's energy.

Scanning electron microscopy was applied to elucidate the effect of grain rotation on grain boundary character distribution by means of the electron channeling pattern method in Ni_3Al, where rotation of six grains with the average rotation angle of 1.1° after final annealing was observed [35]. Electron back-scatter diffraction method was used for the measurement of grain rotation during grain growth in pure polycrystalline aluminum [36]. It was demonstrated that up to a certain temperature grain rotation occurs, which is detected by the increase of the frequency of coincidence grain boundaries. Further increase of temperature results in a reduction of the number of low-energy boundaries and activation of grain boundary migration processes and as a consequence grain growth.

In our previous publication [37], *in situ* measurements of grain rotation during annealing in ultrafine-grained (UFG) aluminum alloy Al-4%Cu-0.5%Zr (wt.%) were performed using single reflection technique, which allows direct determination of orientation of every single grain. In the present paper we continue the study of grain rotation in UFG aluminum alloy Al-4%Cu-0.5%Zr occurring during annealing as a mechanism of structural relaxation accompanied by grain boundary migration and grain growth. Experimental data are then compared to the theoretical results obtained in different approaches.

2. EXPERIMENTAL SETUP

Severe plastic deformation by high pressure torsion (HPT) up to true strain of $e \approx 7$ was used to process an UFG structure in aluminum alloy Al-4%Cu-0.5%Zr. The true strain was calculated from the relationship $e=\ln(\upsilon r/h)$, where υ is the rotation angle (in radians); r and h are the radius and the thickness of the sample, respectively. Investigation and

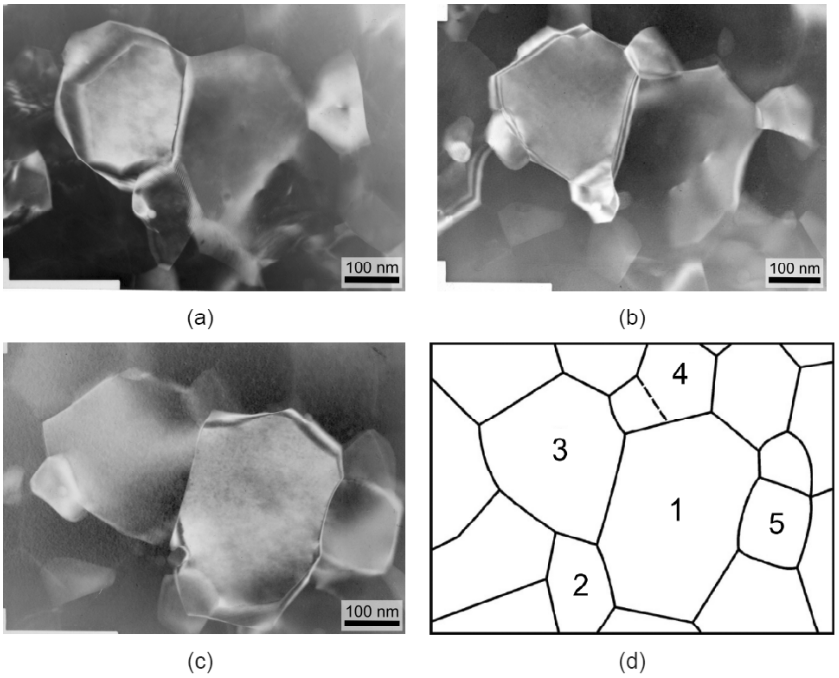

Fig. 1. TEM images of the microstructure of UFG aluminum alloy Al-4%Cu-0.5%Zr: (a) as-prepared state after HPT ($e \approx 7$); after the first (b) and the second (c) anneals for 120 seconds; (d) schematic illustration of the studied region. The dashed line in (d) separates the particle of the second phase from the grain 4.

observation of the sample was carried out in the column of a transmission electron microscope JEM-2000EX with the help of a standard heating device supplied with the microscope. The foils of aluminum alloy were prepared by standard jet electropolishing methods. The area to study was chosen far enough from a foil's edge. An anti-contamination device was applied to reduce the pollution of the foil.

Initially several grain boundary misorientations were measured on the selected region of the as-prepared specimen. The sample was then annealed during 120 seconds at the temperature of 433K and the grain boundary misorientations were measured again. During annealing the studied region was taken out from electron beam to exclude undesirable factors which might have an impact on the observed phenomenon [38]. The selected region was studied on expiry of five minutes after switching off the heating adapter. Thereafter the annealing under the same conditions and the corresponding measurements were repeated. Observation of the microstructure evolution was performed after the first and second anneals. The program of image analysis ImageJ [39] was applied for a determination of the structure modifications during annealing.

Grain boundary misorientations were measured using single reflection technique [40], which is based on a direct measurement of orientation matrix M. The matrix M sets one-to-one correspondence between the laboratory and crystallographic coordinates of the reference vector. Orientation matrix determines the relation between two parallel vectors: (1) unit vector in laboratory coordinate system $r_i(x_i,y_i,z_i)$ and (2) unit vector in reciprocal lattice $g_i(x_i,y_i,z_i)$. The direction toward reciprocal lattice node located on the Ewald sphere, i.e. the reciprocal lattice vector g_i, was chosen for the direction of the reference vector. The orientation matrix M can be determined from the following relation using three non-coplanar unit reference vectors:

$$g_i(h_{i,}k_i,l_i) = M \cdot r_i(x_i,y_i,z_i). \quad (1)$$

The rotation matrix R superposing the crystal lattices of two neighboring grains was calculated from the known orientation matrices of two adjacent grains M_1 and M_2:

$$R = T \cdot M_1 \cdot M_2^{-1}. \quad (2)$$

Here, T is an operator of rotational symmetry of the crystal lattice. Thereafter misorientation angle and misorientation axis were calculated with the help of the elements of the matrix R. For more details, related to the single reflection technique, we refer the reader to Refs. [40,41].

The key feature of the single reflection technique is an ability to determine an orientation of every single grain. Using the orientation matrices of the same grain before and after annealing, misorientation matrix can be calculated and then misorientation

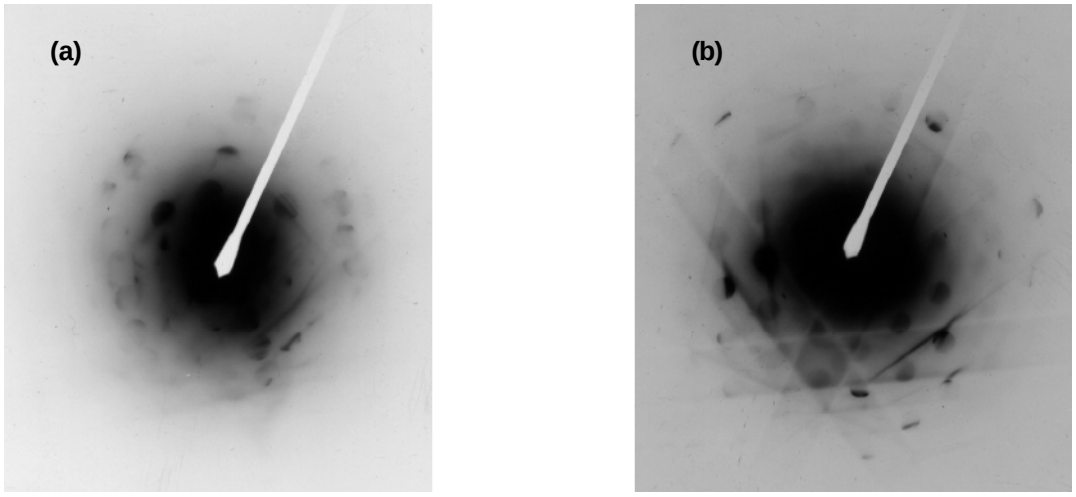

Fig. 2. Electron diffraction patterns of UFG aluminum alloy Al-4%Cu-0.5%Zr obtained by convergent beam electron diffraction in grain No. 1: (a) as-prepared state; (b) after the second annealing.

angle describing rotation of the grain during annealing can be evaluated. The inaccuracy of the orientation measurement for each grain was found to be less than 0.3° and the maximal error in determination of the grain boundary misorientation was less than 0.6°.

3. EXPERIMENTAL RESULTS

Figs. 1a-1c demonstrate TEM images of the microstructure of aluminum alloy Al-4%Cu-0.5%Zr in different states, while Fig. 1d is a schematic representation of the chosen region. The microstructure of the as-prepared aluminum alloy is shown in Fig. 1a. The mean grain size was found to be about 200 nm that is typical for UFG materials prepared by HPT [42]. As seen in Fig. 1a, the grains are dislocation free. However, the presence of extinction contours inside the majority of the grains is an indicator of high internal stresses. The latter statement is also confirmed by convergent beam electron diffraction. Namely, electron diffraction pattern from grain No. 1 in the as-prepared sample does not contain Kikuchi lines as shown in Fig. 2a, while these lines appear after the second annealing (see Fig. 2b). Such a behavior of Kikuchi lines is a clear evidence of long-range internal stresses [43].

Since no dislocation substructure is visible inside the grains, the grain boundaries can be considered as the only sources of these stresses. Two spread dark and light bands seen in the micrographs in Fig. 1a confirm the non-equilibrium state of the grain boundaries, which typically occurs after the absorption of lattice dislocations [42,44].

Five different grain boundaries were studied in the as-prepared state (see Fig. 1a). The boundaries between two grains *n* and *m* were denoted as *n-m*. Dislocation networks were observed at the boundaries 1-2 and 2-3 which have the following misorientations: 18.70° [0.7622, 0.6443, 0.0622] and 54.10° [0.6265, 0.6088, 0.4866], respectively. The boundaries 1-2 and 2-3 were determined to be vicinal to special grain boundaries Σ33a and Σ3, respectively. All results relating to the other boundaries in the selected region are summarized in Table 1. Note that all measured grain boundaries are high-angle ones.

At the end of the first annealing, an increase of the size of grain 1 and no growth of grain 3 were observed (see Fig. 1b). Lattice dislocations were observed in grain 1 only. The second phase particles, which were identified as Al_2Cu, appeared in the triple junctions that is evident from the selected area of electron diffraction patterns taken from grain 4 and its dark-field image shown in Fig. 3. One of these second phase particles has covered grain 2. The emergence of the second phase particles between grains 3 and 4 is accompanied by a disappearance of the grain boundary 3-4. On the scheme of the investigated region (Fig. 1d), the particle of the second phase is separated from grain 4 with the dashed line. Therefore, misorientation of the boundary 3-4 has a conditional character in the sense that such a boundary can exist only in the case if there are somewhere (for instance, in a depth of the foil) regions where grains 3 and 4 contact each other. If such regions do not exist, then this misorientation indirectly shows the change of orientation between grains 3 and 4.

After the first annealing, it became possible to measure the misorientation between grains 1 and 5 (see Table 1). An insignificant migration, when the

Table 1. Summary of the grain boundary misorientations measured in UFG aluminum alloy Al-4 %Cu-0.5 %Zr. The misorientation axis is shown in square parentheses.

State of material	grain boundary misorientation			
	1-3	3-4	1-4	1-5
as-prepared (e = 7)	56.9° [0.728 0.617 0.300]	28.7° [0.944 0.261 0.201]	37.8° [0.853 0.417 0.320]	-
1st annealing at 433K, 120 sec.	58.5° [0.725 0.646. 0.238]	31.2° [0.898 0.325 0.297]	40.1° [0.819 0.476 0.320]	42.2° [0.875 0.384 0.297]
2nd annealing at 433K, 120 sec.	59.0° [0.717 0.617 0.324]	29.8° [0.899 0.346 0.270]	43.3° [0.818 0.504 0.277]	39.1°[0.886 0.368 0.281]

Table 2. Grain rotation after the first and the second anneals.

Change of material state	rotation angle, deg.			
	grain 1	grain 3	grain 4	grain 5
as-prepared → 1st annealing	2.3	2.6	2.4	-
1st annealing → 2nd annealing	1.9	1.4	2.5	2.1

grain boundary of grain 1 moves in the direction of grain 5, was registered.

The first annealing did not lead to an appearance of banded diffraction contrast typical for equilibrium grain boundaries, but dark and light bands became more distinct suggesting a transition to a more equilibrium state (see grain 3 in Fig. 1b). The first annealing was accompanied by a change of the grain boundary misorientations presented in Table 1.

The observed misorientation changes might be related to the appearance of the second phase particles. In order to check that this is not the case, repeated annealing of the sample at similar conditions was carried out. After the second annealing (see Fig. 1c) only insignificant growth of grains 1 and 3 was observed. Diffraction contrast on the grain boundaries became clearer that is an indicator of a further decrease of internal stresses as compared with the first annealing. As seen in Table 1, the misorientation angles of the grain boundaries 1-3, 1-4, and 1-5 are increased. The deviation from this tendency for the boundary 3-4 is related probably to the appearance of the second phase particle.

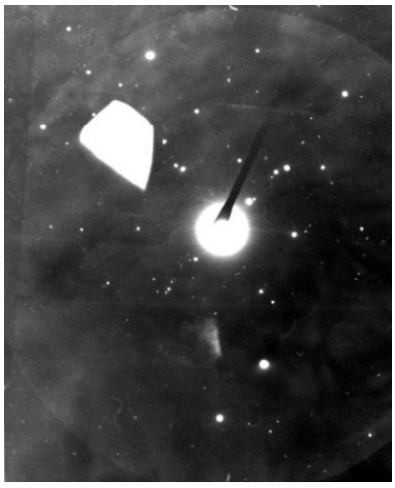

Fig. 3. Selected area of diffraction pattern and dark-field image of the reflex (110) of the second phase particle in grain 4.

The knowledge of orientations of every grain in two different states gives a possibility to calculate the rotation angle between them using the original technique described in Section 2. Thus, rotation angles for grains 1, 3, 4, and 5 during the first and second anneals were calculated and summarized in Table 2.

Visual observations of the microstructure were supplemented by accurate measurements of the grain area and lengths of the grain boundaries, which were performed using image analysis system. Fig. 4 demonstrates the dependence of the area of the studied grains on annealing stages. As seen, grain 1 monotonically grows as the result of the first and the second annealing. Grain 3 begins to grow noticeably only after the second annealing, while no changes were found after the first one. Grain 5 shows only an insignificant growth after the second annealing. The grain boundary length between the grains 1 and 3 in the as-prepared state is 206 nm, after the first annealing it reduces down to 191 nm and then after the second one grows up to 224 nm.

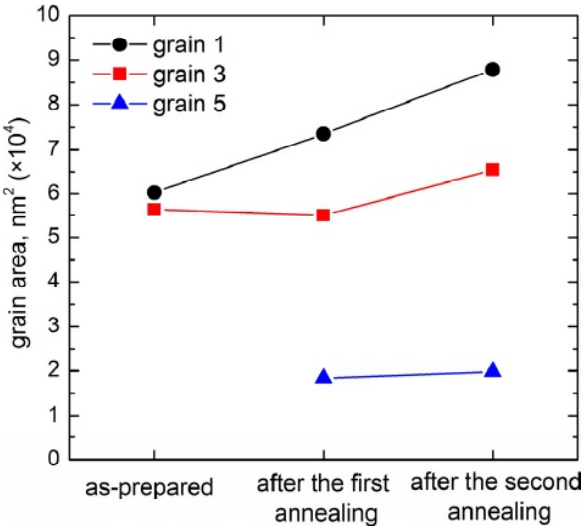

Fig. 4. The area of the grains 1, 3, and 5 in as-prepared state, after the first and the second anneals.

4. DISCUSSION

4.1. Grain rotation

At present, the data on grain rotation during annealing reported in scientific literature are mainly based on a qualitative or indirect characterization of the process [1,31,32,35]. We are not aware of other publications where direct measurements of annealing-induced grain rotation were performed. In our work, the single reflection technique allowed us to characterize quantitatively the change of grain boundary misorientations of every individual grain in the chosen region (see Fig. 1d). Five different nanosized grains surrounded by high-angle grain boundaries were inspected. It was established that grains rotate on angles of 2.3-2.6° and 1.4-2.5° during the first and the second anneals, respectively.

Analysis of the data presented in Table 2 allows us to conclude that after the first annealing grains 1 and 3 (excluding grain 4) rotate by a greater angle than after the second one. Inasmuch as the duration of both annealing processes was the same, it can be concluded that the grain rotation rate gradually decreases with time. A similar result was obtained in thin, fine-grained, columnar <111> textured gold films during sequential annealing [31]. Kuhn et al. [4] have detected that the rotation rate of a single crystal sphere sintered on a single crystal plate decreases with increasing annealing time and after a certain period of time the sphere orientation become independent on time. It occurs due to a reduction of the driving force for rotation, i.e. the grain boundary energy gradient $d\gamma/d\theta$, upon reaching the equilibrium state.

Shibayanagi and co-workers [35] have found that pre-strain effectively enhances grain rotation and average rotation angle (by 2 times) as well as the ratio of rotating grains (by 3 times) in contrast to undeformed specimens. Our interpretation of this fact is that additional strain increases the degree of non-equilibrium of the grain boundaries by means of lattice dislocations absorbed by the grain boundaries. This, in turn, gives rise to an increase of the grain boundary energy gradient with respect to misorientation, i.e. the driving force necessary for grain rotation.

It should be emphasized that non-equilibrium structure of grain boundaries is the main condition of grain rotation occurrence during annealing. The structure of UFG and nanocrystalline materials obtained via severe plastic deformation methods is characterized by high internal stresses arising from grain boundaries, which are in non-equilibrium state [45]. Lattice dislocations trapped by the grain boundaries form non-equilibrium dislocation ensembles [46], which can then relax at elevated temperatures by an escape of extrinsic grain boundary dislocations from the boundary through the adjoining triple junctions [47-50]. Thus, the change of grain boundary misorientation angle and as a consequence a reduction of the excess energy stored in the grain boundaries takes place. Therefore, grain rotation can be considered as a clear indicator of relaxation of non-equilibrium structure in polycrystalline materials.

4.2. Grain growth

Deformation-induced grain growth accompanied by grain rotation and grain boundary migration was intensively studied both experimentally and theoretically [19,51-57]. It was demonstrated that grain growth involved either curvature-driven grain boundary migration or rotation-induced grain coalescence. Since the less the grain size, the larger is the curvature of the boundaries [58], the nanocrystals are *a priori* unstable to grain growth, which can be observed already at relatively low temperatures [59]. Grain coalescence occurs by means of elimination of neighboring subgrains typically delimited by low-angle grain boundaries and consisting of dislocation walls [44,52].

Our observations suggest that annealing-induced grain rotation is also accompanied by grain growth (see Figs. 1 and 4). At that the grains in the studied UFG aluminum alloy are surrounded by high-angle grain boundaries, which are known to have higher mobility in comparison with their low angle counter-

parts [60]. In these circumstances, no coalescence of the grains with vicinal orientations takes place and therefore grain boundary migration driven mechanism of grain growth is supposed to be dominant. Shortening of total length of non-equilibrium grain boundaries via migration naturally results in a reduction of internal stresses. Besides, the anisotropy of the stored elastic energy in grains can be an additional factor influencing the grain boundary migration and grain rotation [44]. On the other hand, Lian et al. [61] have shown that non-equilibrium grain boundaries in materials prepared by high pressure torsion possess high mobility, which significantly facilitates grain growth. Thus, in our case, grain growth occurring by means of grain boundary migration at elevated temperatures can be considered as an evidence of relaxation of non-equilibrium structure.

4.3. Comparison with theoretical studies

It is well-known that plastic deformation stimulates the movement of lattice dislocations toward grain boundaries, which are known to be effective sinks for them. It leads to a change of the misorientation angle, an appearance of excess elastic energy and long-range stress fields. Since all grains are dislocation free after severe plastic deformation, then it allows us to assume that prior TEM observation all lattice dislocations are absorbed by the grain boundaries, which are in a non-equilibrium state. Therefore, grain rotation during subsequent annealing should occur due to a rearrangement of these trapped lattice dislocations, which thereafter can leave the boundary and thus change the misorientation angle.

Theoretical studies of the kinetics of grain rotation were performed in both discrete-dislocation and continuum approaches. In discrete-dislocation approach the kinetics is controlled by the climb velocity of the dislocations under the forces of elastic interactions, while continuum approach considers a diffusive transport of matter from the compressive regions into the tensile ones. Below we calculate the rotation time in these two approaches using experimental data for the boundary 1-3. This boundary was chosen due to its straightness and an absence of the second phase particles.

The kinetics of grain rotation in the discrete-dislocation approach was investigated in a bicrystal containing a tilt grain boundary by a consideration of the relaxation of an edge dislocation wall [50]. It was found that the relaxation time to reach the metastable configuration for a given film thickness is proportional to the logarithm of the misorientation angle and can be written in the following way:

$$t_f = \frac{\pi(1-\nu)kTL^3}{2\delta D_b G\Omega}\cdot\left[-2.68+1.04\ln\left(\frac{L\theta}{2b}\right)\right], \qquad (3)$$

where D_b refers to the grain boundary diffusion coefficient; δ is the diffusiion width of the boundary; G and ν are the shear modulus and Poisson's ratio, respectively; Ω is atomic volume; k is Bolzmann's constant; T is temperature; L is thickness of the film infinitely extended along the dislocation line; b is the magnitude of the Burgers vector of dislocations normal to the boundary plane and the dislocation line; θ is misorientation angle of the tilt grain boundary. Despite the fact that dislocation wall considered in Ref. [50] is equivalent to small-angle grain boundary, the results of the cited paper can be extended for the high-angle grain boundaries, which are vicinal to the special misorientation due to the fact that the structure of such boundaries can be described as a network of grain boundary dislocations imposed on the special grain boundary. For our rough estimation we use the following parameters for pure aluminum: G=26 GPa, ν=0.35, the lattice constant a=0.405 nm, L=225 nm (obtained from Fig. 1), grain boundary diffusion constants δD=5.0x10^{-14} exp(84000/RT) m^3 s^{-1} [62]. The symbol R denotes the gas constant. Computation gives circa 60 seconds. Taking into account the approximate nature of the qualitative comparison, we can conclude that our estimates are in a good agreement with the experimental data presented above.

The kinetics of grain rotation in continuum approach was considered in Ref. [31]. It was assumed that the driving force for grain rotation is provided by the aggregate energy gradient with respect to misorientation. The authors of [31] obtained the following expression for rotation rate:

$$\frac{d\theta}{dt} = \frac{128\delta D_b\Omega}{kTL^4}\cdot\sum_i\left(\frac{d\gamma_i}{d\theta}\right), \qquad (4)$$

where the aggregate energy gradient $\Sigma_i(d\gamma_i/d\theta)$ was taken to be 1/15 J/m^2 per degree of arc on the basis that grain boundary energy rises from zero to a value of the order of 1.0 J/m^2 over the range from 0° to 15° of misorientation. Transforming the infinitesimal increments to the finitesimal ones, we can evaluate the time necessary for the grain boundary 1-3 to rotate on the angle of $\Delta\theta$=2.1° as

$$\Delta t = \frac{kTL^4}{128\delta D_b \Omega} \cdot \frac{\Delta\theta}{\sum_i \left(\frac{d\gamma_i}{d\theta} \right)}. \quad (5)$$

Using the same values of the parameters, we obtain 6.7×10^4 seconds. This is two orders of magnitude larger than that calculated with formula (3). Thus, discrete-dislocation approach gives better estimate of grain rotation time in UFG materials in contrast to continuum model.

5. CONCLUSIONS

The experimental procedure based on the single reflection technique allowed us to determine orientations of individual grains of a UFG polycrystal and calculate angles of their rotations, which occur during *in situ* TEM annealing. Short-time annealing of UFG aluminum alloy Al-4%Cu-0.5%Zr prepared by HPT technique results in a change of grain boundary misorientations, i.e. grain rotation accompanying with a simultaneous grain growth. Experimentally observed changes of grain boundary misorientations, both grain rotation and grain growth can be directly associated with the relaxation processes and transition to a more equilibrium state. Theoretical estimates for the rotation time made in the discrete-dislocation approach are consistent with the obtained experimental data.

ACKNOWLEDGEMENT

The work was performed using the facilities of the shared services center of the Institute for Metals Superplasticity Problems of Russian Academy of Sciences «Structural and Physical-Mechanical Studies of Materials». Support of Federal Agency of Scientific Organizations under the State Assignement Theme No. 0060-2016-0001 is acknowledged.

REFERENCES

[1] H. Hu, *Recovery and Recrystallization of Metals* (Wiley, New York, 1963).
[2] J.C.M. Li // J. *Appl. Phys*. **33** (1962) 2958.
[3] G. Herrmann, H. Gleiter and G. Baro // *Acta. Metall. Mater*. **24** (1976) 353.
[4] H. Kuhn, G. Baero and H. Gleiter // *Acta. Metall. Mater*. **27** (1979) 959.
[5] H. Mykura // *Acta. Metall. Mater.* **27** (1979) 243.
[6] S.W. Chan and R.W. Balluffi // *Acta Metall. Mater*. **33** (1985) 1113.
[7] S.W. Chan and R.W. Balluffi // *Acta Metall. Mater*. **34** (1986) 2191.
[8] M. Ke, S.A. Hackney, W.W. Milligan and E.C. Aifantis // *Nanostructr. Mater*. **5** (1995) 689.
[9] P. Liu, S.C. Mao, L.H. Wang, X.D. Han and Z. Zhang // *Scripta Mater*. **64** (2011) 343.
[10] F. Mompiou and M. Legros // *Scripta Mater*. **99** (2015) 5.
[11] E. Izadi, A. Darbal, R. Sarkar and J. Rajagopalan // *Mater. Design* **113** (2017) 186.
[12] N. Yagi, A. Rikukawa, H. Mizubayashi and H. Tanimoto // *Mater. Sci. Eng. A* **442** (2006) 323.
[13] N.I. Noskova and E.G. Volkova // *Phys. Metals Metallogr.* **91** (2001) 629.
[14] Y.T. Zhu, X.Z. Liao and X.L. Wu // *Progr. Mater. Sci.* **57** (2012) 1.
[15] I.A. Ovid'ko and E.C. Aifantis // *Rev. Adv. Mater. Sci*. **35** (2013) 1.
[16] N.Y. Zolotorevsky, Y.F. Titovets and G.Y. Dyatlova // *Scripta Mater.* **38** (1998) 1263.
[17] H.F. Poulsen, L. Margulies, S. Schmidt and G. Winther // *Acta Mater.* **51** (2003) 3821.
[18] P. Chen, S.C. Mao, Y. Liu, F. Wang, Y.F. Zhang, Z. Zhang and X.D. Han // *Mater. Sci. Eng. A* **580** (2013) 114.
[19] T. Gorkaya, K.D. Molodov, D.A. Molodov and G. Gottstein // *Acta Mater*. **59** (2011) 5674.
[20] G.K. Tirumalasetty, M.A. van Huis, C. Kwakernaak, J. Sietsma, W.G. Sloof and H.W. Zandbergen // *Acta Mater.* **60** (2012) 1311.
[21] M.W. Bird, P.F. Becher and K.W. White // *Acta Mater.* **89** (2015) 73.
[22] W.S. Li, H.Y. Gao, H. Nakashima, S. Hata and W.H. Tian // *Mater. Sci. Eng. A* **649** (2016) 417.
[23] R. Goswami, S.B. Qadri and C.S. Pande // *Acta Mate*r. **129** (2017) 33.
[24] J.C. Stinville, J. Cormier, C. Templier and P. Villechaise // *Acta Mater.* **83** (2015) 10.
[25] O.A. Kaibyshev, *Superplasticity of Alloys, Intermetallides and Ceramics* (Springer-Verlag, Berlin, 1992).
[26] A. Vevecka and T.G. Langdon // *Mater. Sci. Eng. A* **187** (1994) 161.
[27] J. Koike, M. Mabuchi and K. Higashi // *Acta Metall. Mater.* **43** (1995) 199.
[28] W. Beere // *Philos T R Soc A* **288** (1978) 177.
[29] V. Paidar and S. Takeuchi // *J. Phys. III* **1** (1991) 957.

[30] L. Margulies, G. Winther and H.F. Poulsen // *Science* **291** (2001) 2392.
[31] K.E. Harris, V.V. Singh and A.H. King // *Acta Mater*. **46** (1998) 2623.
[32] F.J. Humphreys and H.M. Chan // *Mater. Sci. Technol.* **12** (1996) 143.
[33] V. Randle // *Mater. Sci. Technol.* **7** (1991) 985.
[34] V. Randle and B. Ralph // *J. Mater. Sci.* **22** (1987) 2535.
[35] T. Shibayanagi, K. Sumimoto and Y. Umakoshi // *Scripta Mater.* **34** (1996) 1491.
[36] T. Yamasaki, Y. Demizu and Y. Ogino // *Mater. Sci. Forum* **204-206** (1996) 461.
[37] V.N. Danilenko, D.V. Bachurin and R. Mulyukov // *Letters on materials* **4** (2014) 233.
[38] P.S. Sklad and T.E. Mitchell // *Acta Metall. Mater*. **23** (1975) 1287.
[39] C.A. Schneider, W.S. Rasband and K.W. Eliceiri // *Nature Methods* **9** (2012) 671.
[40] V.V. Rybin, *Large Plastic Deformations and Fracture of Metals* (Metallurgiya, Moscow, 1986).
[41] R.Z. Valiev, A.N. Verzgazov and V.Y. Gertsman, *Crystal-Geometrical Analysis of Intercrystallite Boundaries in the Practice of Electron Microscopy* (Nauka, Moscow, 1991).
[42] R.Z. Valiev, A.P. Zhilyaev and T.G. Langdon, *Bulk Nanostructured Materials: Fundamentals and Applications* (Wiley, Hoboken, 2013).
[43] G. Thomas and M.J. Goringe, *Transmission Electron Microscopy of Materials* (John Wiley & Sons, New York, 1979).
[44] A.J. Haslam, S.R. Phillpot, H. Wolf, D. Moldovan and H. Gleiter // *Mater. Sci. Eng. A* **318** (2001) 293.
[45] A.A. Nazarov and R.R. Mulyukov, In: *Handbook of Nanoscience, Engineering, and Technology* (CRC Press, Boca Raton, 2003), p. 22-1.
[46] A.A. Nazarov, A.E. Romanov and R.Z. Valiev // *Scripta Mater.* **34 (**1996) 729.
[47] D.V. Bachurin and A.A. Nazarov // *Philos. Mag*. **83** (2003) 2653.
[48] A.A. Nazarov // *Interface Sci*. **8** (2000) 315.
[49] A.A. Nazarov and D.V. Bachurin // *Phys. Metals Metallogr*. **96** (2003) 446.
[50] D.V. Bachurin, A.A. Nazarov and J. Weissmuller // *Acta Mater.* **60** (2012) 7064.
[51] D. Moldovan, D. Wolf and S.R. Phillpot // *Acta Mater.* **49** (2001) 3521.
[52] D. Moldovan, D. Wolf and S.R. Phillpot, A.J. Haslam // *Acta Mater*. **50** (2002) 3397.
[53] Z.T. Trautt and Y. Mishin // *Acta Mater.* **60** (2012) 2407.
[54] Z.T. Trautt and Y. Mishin // *Acta Mater.* **65** (2014) 19.
[55] M. Upmanyu, R.W. Smith and D.J. Srolovitz // *Interface Sci.* **6** (1998) 41.
[56] M. Upmanyu, D.J. Srolovitz, A.E. Lobkovsky, J.A. Warren and W.C. Carter // *Acta Mater.* **54** (2006) 1707.
[57] M. Jin, A.M. Minor, E.A. Stach and J.W. Morris // *Acta Mater.* **52** (2004) 5381.
[58] C. Herring, In: *The Physics of Powder Metallurgy*, ed. by W.E. Kingston, (New York: McGraw-Hill, 1951), p. 143
[59] H. Gleiter // *Progr Mater. Sci.* **33** (1989) 223.
[60] F.J. Humphreys and M. Hatherly, *Recrystallization and Related Annealing Phenomena* (Pergamon, Oxford, 1995).
[61] J.S. Lian, R.Z. Valiev and B. Baudelet // *Acta Metall. Mater*. **43** (1995) 4165.
[62] I. Kaur, W. Gust and L. Kozma, *Handbook of Grain and Interphase Boundary Diffusion Data* (Ziegler Press, Stuttgart, 1989).